This article was downloaded by:
On: *26 January 2011*
Access details: *Access Details: Free Access*
Publisher *Taylor & Francis*
Informa Ltd Registered in England and Wales Registered Number: 1072954 Registered office: Mortimer House, 37-41 Mortimer Street, London W1T 3JH, UK

Liquid Crystals
Publication details, including instructions for authors and subscription information:
http://www.informaworld.com/smpp/title~content=t713926090

Multilayered crystalline structures and liquid crystalline phases in a mesogen with siloxane tails

Cary A. Vieth[ab]; Edward T. Samulski[a]; N. Sanjeeva Murthy[c]
[a] Department of Chemistry, University of North Carolina, Chapel Hill, North Carolina, U.S.A. [b] Shell Development Co., Westhollow Technology Center, Houston, Texas, U.S.A. [c] AlliedSignal Inc., Research and Technology, Morristown, New Jersey, U.S.A.

To cite this Article Vieth, Cary A. , Samulski, Edward T. and Murthy, N. Sanjeeva(1995) 'Multilayered crystalline structures and liquid crystalline phases in a mesogen with siloxane tails', Liquid Crystals, 19: 5, 557 — 563
To link to this Article: DOI: 10.1080/02678299508031068
URL: http://dx.doi.org/10.1080/02678299508031068

PLEASE SCROLL DOWN FOR ARTICLE

Full terms and conditions of use: http://www.informaworld.com/terms-and-conditions-of-access.pdf

This article may be used for research, teaching and private study purposes. Any substantial or systematic reproduction, re-distribution, re-selling, loan or sub-licensing, systematic supply or distribution in any form to anyone is expressly forbidden.

The publisher does not give any warranty express or implied or make any representation that the contents will be complete or accurate or up to date. The accuracy of any instructions, formulae and drug doses should be independently verified with primary sources. The publisher shall not be liable for any loss, actions, claims, proceedings, demand or costs or damages whatsoever or howsoever caused arising directly or indirectly in connection with or arising out of the use of this material.

LIQUID CRYSTALS, 1995, VOL. 19, NO. 5, 557–563

Multilayered crystalline structures and liquid crystalline phases in a mesogen with siloxane tails

by CARY A. VIETH† and EDWARD T. SAMULSKI*
Department of Chemistry, University of North Carolina, Chapel Hill, North Carolina 27599-3290, U.S.A

and N. SANJEEVA MURTHY*
AlliedSignal Inc., Research and Technology, Morristown, New Jersey 07962-1021, U.S.A.

(*Received 24 April 1995; accepted 23 May 1995*)

N,N'-Terephthalylidine-bis-4-(2 pentamethyldisiloxyethyl)aniline, TBS2A, which contains a mesogenic group with two di-siloxane tails, and TBS3A with two tri-siloxane tails were synthesized. Liquid crystalline behaviour in these compounds were studied by DSC and polarized light microscopy. Temperature-induced structural transitions in TBS2A were studied using variable temperature X-ray diffraction. At least three structural phase transitions were observed: crystal–crystal transformation (from Cr2 to Cr3) at 125°C, crystalline phase (Cr3) to a smectic liquid crystalline phase (S_B) at 140°C, and the melting of the S_B phase at 152°C. A room temperature crystalline phase (Cr1) with a layer repeat of 29·5 Å is also observed. The low temperature Cr2 phase is characterized by a layer repeat of 26·3 Å and exhibits a long spacing of 105 Å corresponding to a repeat unit of four layers. The high temperature Cr3 phase has a layer repeat of 22·2 Å and exhibits a long spacing of 44 Å from a repeat unit with two layers. The mesophase has a single layer with a repeat of 22·2 Å. The di-siloxane tails in the Cr3 and the mesophase are fully interdigitated. The isotropic melt shows a diffuse halo at 24 Å corresponding to the separation of adjacent layers, and a second halo at 6·5 Å attributed to the separation of the mesogens/chains within the layers. These results are interpreted with structural models.

Downloaded At: 09:41 26 January 2011

1. Introduction

When siloxanes are substituted for alkanes in calamitic liquid crystals (LCs), the transition temperatures are reduced along with the temperature range of mesophase stability, or the mesophase may be eliminated altogether depending on the nature of the mesogen [1–4]. This is due in part to the increased bulkiness and flexibility of the siloxane moieties which reduces their packing efficiency relative to their alkane counterparts. On the other hand, because of the intrinsic incompatibility between the siloxane tails and the hydrocarbon mesogenic core, there is a competing stabilizing aspect of siloxane-substituted mesogens: a propensity for nanophase separation of the chemically distinct components results in better delineated layered (smectic) structure comprised of siloxane-rich and hydrocarbon-rich strata [5]. To gain a better understanding of this phenomenon, we have studied the various types of lamellae structures exhibited by a model compound consisting of two siloxane chains attached to each end of the prolate core *N,N'*-terephthalylidene-bis-4-vinylaniline (TBVA), itself a mesogen. The resulting new liquid crystal, *N,N'*-terephthalydine-bis-4-(2'-pentamethyldisiloxyethyl)aniline (TBS2A), exhibits a smectic B mesophase. Here we report the synthesis, optical studies, thermal analysis and variable temperature X-ray diffraction (XRD) data on this siloxane-substituted mesogen.

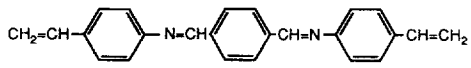

TBVA

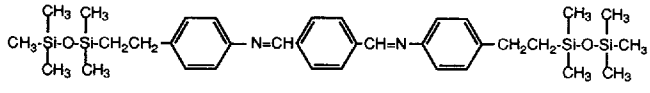

TBS2A

The thermal and optical work shows the following transitions for the TBS2A mesogen: Cr 138°C S_B 152°C I. The optical characteristics of the mesophase between 138°C and 152°C are those of a smectic B (S_B)

* Authors for correspondence.
† Present address: Shell Development Co., Westhollow Technology Center, P.O. Box 1380, Houston, Texas 77251-1380, U.S.A.

0267–8292/95 $10·00 © 1995 Taylor & Francis Ltd.

Table 1. Thermal transitions of the siloxane mesogens.

Compound	Transition temperatures/°C	ΔH/kJ mol^{-1}	ΔS/J mol^{-1} K^{-1}
TBVA	Cr1 95 Cr2 180 N [pzn]	3·5, 4·7	9·5, 10·4
TBS2A	Cr 142 S_B 152 I	8·7, 38·4	21·2, 90·8
TBS3A	Cr 77 (S_B) 83 I	5·9, 30·4	16·9, 85·4

pzn, Polymerization; Cr, Crystalline; I, Isotropic.

phase. This is confirmed by the observation that TBS2A is miscible with a known S_B mesogen, *trans*-1,4-cyclohexane-di-4′-*n*-octyloxybenzoate (CDOB). X-ray scattering experiments were carried out to confirm the S_B phase and to study the structural features of the crystalline and LC phases.

2. Experimental

2.1. *Synthesis*

The precursor mesogen TBVA was prepared by the acetic acid catalysed condensation of 1 mol of terephthaldicarboxaldehyde and 2 mols of *p*-aminostyrene in ethanol solvent at 0–50°C. Purification was by recrystallization from ethyl acetate and ^{1}H NMR confirmed the structure (δ (ppm): 8·5 (singlet, 2 H), 8·0 (singlet, 4 H), 7·4 (doublet, 4 H), 7·2 (doublet, 4 H), 6·7 (quartet, 2 H), 5·7 (doublet, 2 H), 5·2 (doublet, 2 H).

TBS2A was prepared by attaching siloxane tails to TBVA. In the synthesis, both 1,1,1,3,3-pentamethyldisiloxane ($H–Si(CH_3)_2–O–Si(CH_3)_3$, PMDS) and 1,1,1,3,3,5,5-heptamethyltrisiloxane, ($H–Si(CH_3)_2–O–Si(CH_3)_2–O–Si(CH_3)_3$, HpMTS) were each hydrosilated separately to the TBVA using dicyclopentadienyl platinum dichloride (DCP/Pt) catalyst in tetrahydrofuran (THF) (or alternatively toluene) at 60–90°C. The catalyst was prepared according to the procedure of Drew and Doyle [6]. ^{1}H NMR confirmed the desired structure for TBS2A (δ (ppm): 8·55 (singlet, 2 H), 8·0 (singlet, 4 H), 7·25 (quartet(?), 8 H), 2·65 (quintet, 4 H), 0·9 (quintet, 4 H), 0·1 (singlet, 30 H).

The second siloxane-based mesogen, *N,N′*-terephthalylidine-bis-4-(2′-heptamethyltrisiloxyethyl(aniline) (TBS3A), exhibited similar NMR spectral features (δ (ppm): same as TBS2A except for 42 H at *c.* 0·1 ppm).

2.2. *X-ray diffraction (XRD)*

Data were collected using a 1-D position sensitive detector mounted on a Franks camera with slitless, focusing optics using Ni-filtered CuK_α radiation. The sample to detector distance was set at ~ 33 cm for small angle scans (max $2\theta = 7°$) and at ~ 12 cm for medium-angle scans (max $2\theta = 22°$); the detector channels were calibrated using lead stearate. The sample was mounted in an X-ray quartz capillary. The temperature was varied by directing a stream of heated air over the capillary and the actual temperature was measured with a thermocouple placed close to the sample. Data were collected for 1 min to 1 h depending on the scattered intensity.

2.3. *DSC*

Scanning calorimetry was obtained on a DuPont 9900 instrument with a 3·4 mg sample using a scan rate of 10°C min^{-1}.

3. Results and discussion

The prominent thermal transition temperatures, and the corresponding entropies and phase designations of all of the mesogens are reported in table 1. The precursor mesogen, TBVA shows a solid–solid transition at *c.* 95°C and melts into a nematic mesophase at 180°C which then thermally polymerizes.

The bis-siloxane terminated-TBVA, TBS2A, exhibited a solid to smectic transition (see below) at 142°C. This melting transition is substantially lower than the 180°C transition from crystal to nematic seen in the precursor

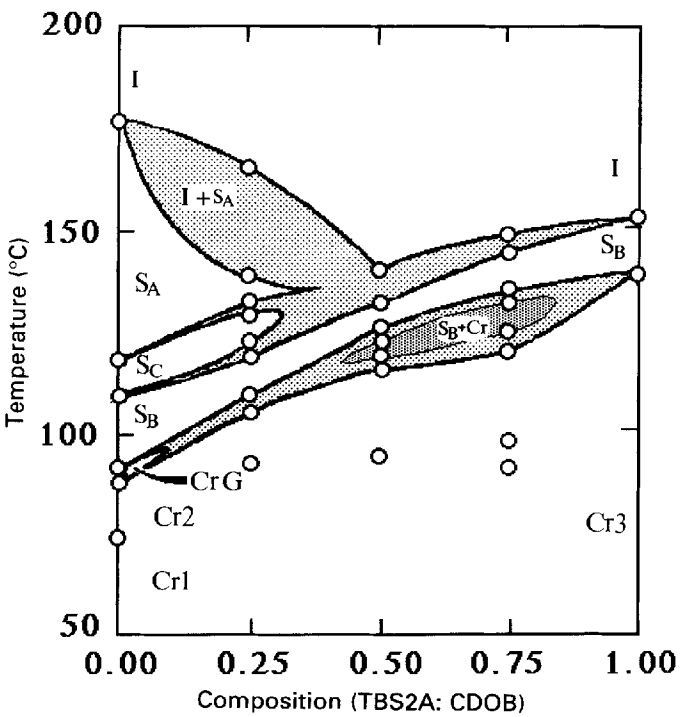

Figure 1. Temperature–composition phase diagram for the miscibility of TBS2A and CDOB.

Downloaded At: 09:41 26 January 2011

mesogen, TBVA. The lowering of the transition temperature is due to incorporation of flexible Si–O linkages and has been seen for other polysiloxane Schiff's base side chain LC polymers (see, for example, [7, 8]) and main chain siloxane LC polymers [9]. The mesophase of TBS2A between 142 and 151°C showed crystal-like features characteristic of the S_B mesophase. The formation of such a stable smectic mesophase is undoubtedly due to the strong thermodynamical compatibility of the siloxane terminal chains with the hydrocarbon constituents of the (TBVA) mesogenic core. This incompatibility would favour nanophase separation which in turn, would reinforce smectic LC formation.

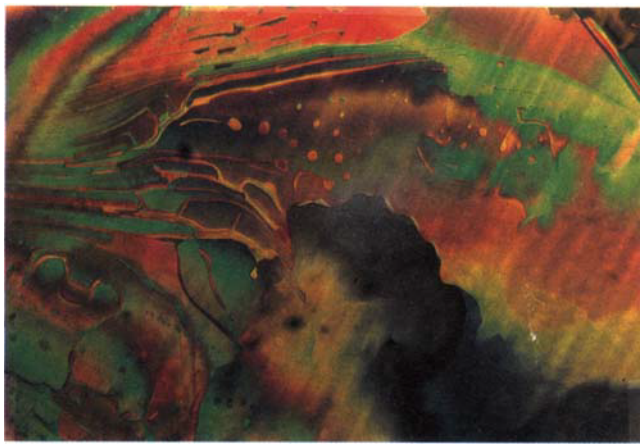

(*a*)

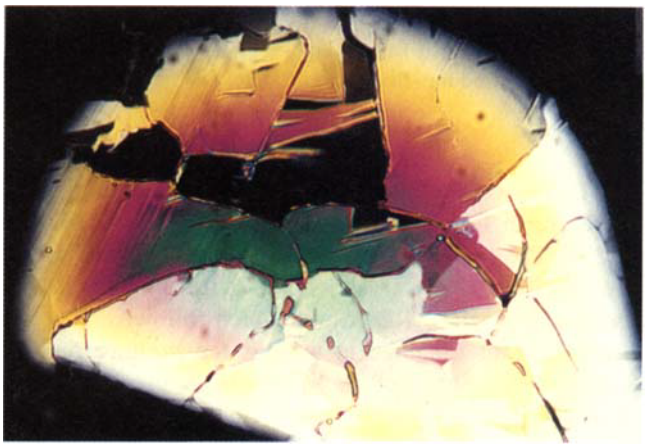

(*b*)

Figure 2. Polarized optical micrographs for TBS2A. (*a*) Mosaic texture of TBS2A melt; $T = 151$°C; magnification 160 ×. (*b*) High magnification view of thin film S_B mosaic texture of TBS2A, $T = 149$°C; magnification 640 ×.

The phase designation of TBS2A has been studied in detail through miscibility studies with a second mesogen, CDOB [10], which exhibits the following transitions: Cr 90°C G 93°C S_B 111°C S_C 119°C S_A 178°C I [10, 11]. Three blends containing 25, 50 and 75 wt % of TBS2A with CDOB were prepared and analysed by DSC and optical polarizing microscopy to construct the phase diagram shown in figure 1. This shows that the S_B phase is miscible across the entire composition range indicating that the smectic phase in TBS2A is a S_B phase. At 25 wt % of TBSA in CDOB (the 25/75 blend), three liquid crystalline regions exist, smectic A, C and B with a broad two phase region prior to clearing at 165°C. With the 50/50 and 75/25 blends, one LC phase is discernible when cooled from the isotropic liquid. For the 50/50 blend, the LC phase exhibits a typical S_B mosaic texture [12]. For the blend with 75 wt % TBS2A, the mosaic texture is again seen in the LC phase upon cooling from the isotropic melt. Upon further cooling, a rather abrupt change occurs at ~ 130–132°C where the material appears to exhibit biphasic behaviour with a crystalline solid coexisting with a LC S_B. Some regions of this blend exhibit a mosaic texture very similar to the pure TBS2A texture shown in figure 2(*a*), whereas the other regions appear to contain two phases. This is depicted as the shaded regions in figure 1, labelled (S_B + Cr).

The mosaic texture of TBS2A is shown in figures 2 (*a*) and (*b*), the former is a thicker specimen between cover slips and resembles the samples used in the miscibility analyses in both texture and colour. The latter is a very thin film preparation of TBS2A and shows the mosaic texture of S_B formed from the isotropic melt. The region in the centre is homeotropic as it remains black when the

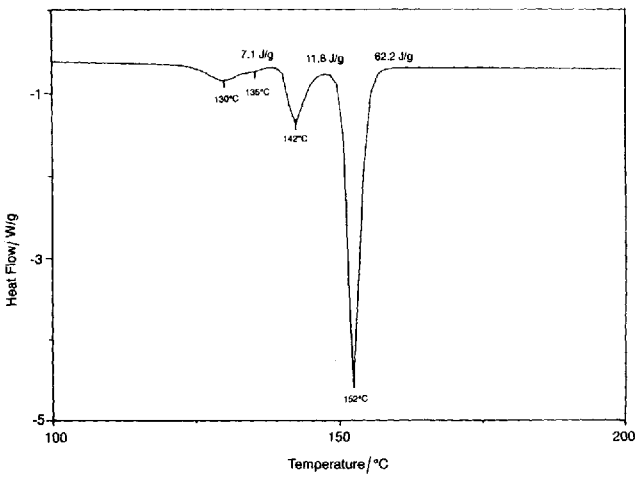

Figure 3. A DSC scan showing TBS2A solid state transitions at 130°C (and 135°C) and the solid-to-mesophase transition at 142°C followed by melting into the isotropic state at 152°C.

Downloaded At: 09:41 26 January 2011

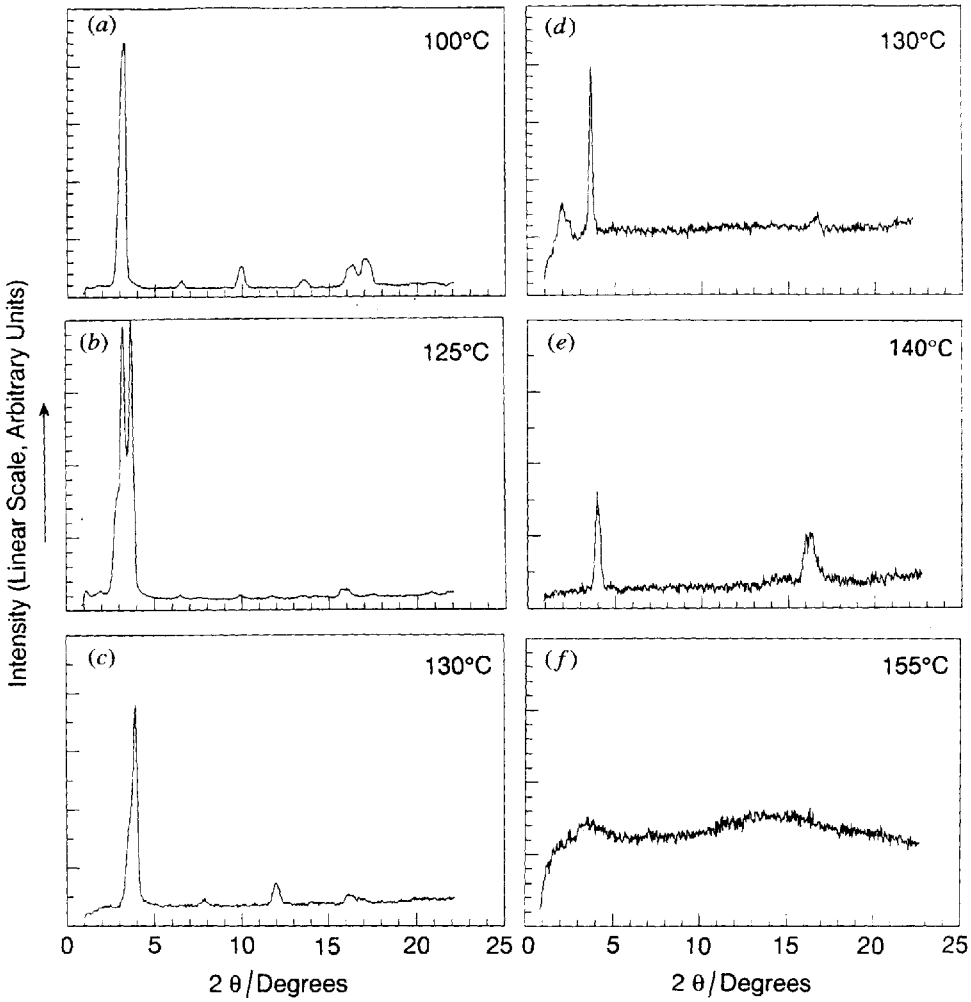

Figure 4. XRD scans obtained at various temperatures; *d*-spacings of the diffraction peaks are given in table 2: (*a*) 100°C—this shows up to four orders of the 26·3 Å spacing along with a 50 Å peak, Cr2; (*b*) 125°C—this scan shows the coexistence of all the three crystalline phases, Cr1, Cr2 and Cr3; (*c*) 130°C—the Cr3 phase appears as the dominant phase along with a trace of Cr2; (*d*) 130°C—shows the low angle 44 Å peak; (*e*) 140°C—this scan was obtained when the sample was flowing and just before it melted into the isotropic state; (*f*) 155°C—this scan was obtained in the isotropic melt.

Downloaded At: 09:41 26 January 2011

analyser and polarizer are rotated in unison. According to Gray and Goodby [13], mosaic areas of S_B compounds have a typical 'H' shape and this can be seen in the centre platelet of TBS2A in figure 2 (*b*).

The second mer, TBS3A, containing twin trisiloxane tails continues the expected trend of lower transition temperatures and stability ranges with greater siloxane content. However, here the range of the LC phase is only several degrees and the two transition endotherms are not separable by DSC. We identify the short-ranged LC phase as S_B due to formation of a mosaic texture at 79–80°C just before crystallization; this texture is very similar to that of TBS2A.

When we look in more detail at the thermal properties of TBS2A, we see that in the DSC scan given in figure 3 there are in fact four endotherms at 130, 135, 142 and 152°C. The first two minor transitions at 130 and 135°C are attributed to crystal–crystal transformations as evidenced by the XRD results which follow.

XRD scans obtained at various temperature regimes selected on the basis of the DSC data are given in figures 4 (*a*)–(*f*), and the results are summarized in table 2. Not shown in the table are the long spacings at 50 Å and 95–110 Å which were occasionally observed (see figure 5). TBS2A crystallizes as thin platelets, and hence the sample capillary was rotated by an arbitrary angle between the scans (thus changing the angle between the plate-normal and the incident X-rays) to capture both the

Table 2. *d*-spacings observed for crystal (Cr), liquid crystal (LC) and isotropic melt.

		Diffraction spacings/Ångstroms												
		Interlayer peaks									Intralayer peaks			
Temperature/°C	Phases	44	35	30	26	23	13·6	11·2	8·8	7·5	6·5	5·6	5·5	5·2	Figure
	Cr1			1											
	Cr2				1		2		3		4				
	Cr3	1				2		4		6					
22				●	●								●–	●–	
				●					●●				●●	●	
		●			●		●		●		●			●–	
		●			●	●		●		●			●		
70		●			●		●		●		●●				
					●								●	●●	
				●					●				●		
100		●			●		●		●		●		●●	●	4(*a*)
					●								●	●	
					●				●		●●		●		
125					●	●	●		●		●		●		
		●		●	●	●	●		●	●	●	●●		●	4(*b*)
					●	●						●		●	
					●	●						●	●	●–●–	
		●			●	●						●	●		
						●		●		●		●	●	●	
		●	●			●						●	●	●	
		●	●			●							●		4(*d*)
						●		●		●					
140					●	●					●●			●	
					●	●		●		●				●	4(*c*)
					●	●						●	●		
	LC														
140+						22							5·4		4(*e*)
	Melt														
150–205						24						6·6			4(*f*)

Numbers 1–6 shown for the Cr1, Cr2 and Cr3 phases are the various orders of the Bragg reflection. The filled circles indicate the presence of a diffraction peak in a particular run. Two circles indicate a closely spaced (within ~0·1 Å) doublet. A minus sign indicates *d*-spacings which are ~0·1 Å less than the column value. The positions of the peaks in the LC phase and the melt are different from those of the crystalline phases and hence their actual *d*-spacings are given in the table.

interlayer and the intralayer peaks. In doing so, we found that the 5·5 and 5·2 Å reflections are clearly due to lateral packing of the chains. We suspect there is some contribution from the lateral packing of the chains to the 6·5 and 5·6 Å reflections as well. All the other peaks are most likely due to interlayer reflections.

The XRD data summarized in table 2 enable us to identify at least five different structures in TBS2A: three crystalline structures (Cr1, Cr2 and Cr3), a liquid crystalline phase and the melt. The three crystalline phases are characterized by layer repeats of 29·5, 26·3 and 22·2 Å, respectively. The liquid crystalline phase has a layer repeat of 22·2 Å. A diffuse halo at ~24 Å in the melt suggests that the layered (nanophase-separated) organization of the TBS2A molecules is maintained in the isotropic melt even at temperatures as high as 200°C. The endotherms observed between 125 and 140°C correspond to the crystalline phase transition between Cr2 and Cr3. The 140°C endotherm represents the transformation of the Cr3 crystalline phase into the S_B liquid crystalline phase which eventually melts into an isotropic phase at 152°C.

Structural models to explain the diffraction data from the various phases are shown in figure 6. Starting with the energy minimized mesogen molecular structure (shown edge-on in figure 6(*a*)), we can envision two types of interaction between the siloxane tails: close-packing versus interdigitated. Siloxane moieties on neighbouring molecules can be packed next to each other resulting in a layer spacing of 30 Å corresponding to the Cr1 structural data (see figure 6(*b*)). The Cr1 phase appears to be disordered since no higher order reflections of the layer repeat were observed.

Interdigitation of the siloxane tails on neighbouring molecules yields a layer spacing of < 30 Å which we have

Downloaded At: 09:41 26 January 2011

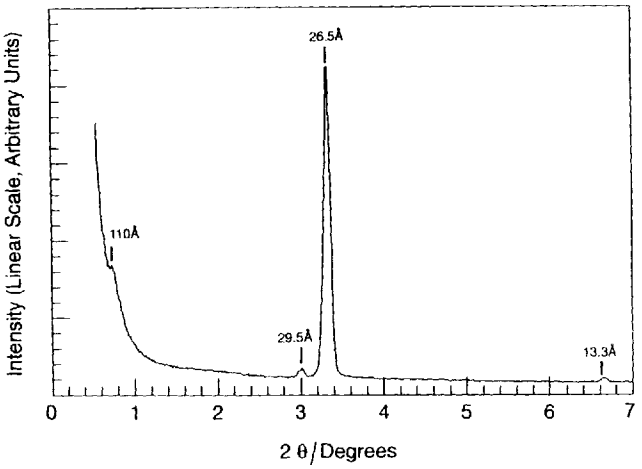

Figure 5. An XRD scan (22°C) to show the low angle peak at ~ 110 Å.

identified as Cr2 and Cr3 phases (see figure 6(*c*)). The XRD scans of the low temperature crystalline phases (Cr2; $T < 125$°C) are shown in figures 4(*a*) and (*b*). The Cr2 phase is highly ordered since it shows at least 4 orders of an interlayer repeat of 26·3 Å. The XRD scans of the high temperature crystalline phase (Cr3; 125°C $< T <$ 140°C) are shown in figures 4(*b*)–(*d*). Although a single low angle peak with $d = 23$ Å is sometimes observed for Cr3, most frequently a peak at 22·2 Å appears along with at least three higher order reflections. Hence the Cr3 phase, like Cr2, is highly ordered.

In general, Cr1 and Cr2 phases can be regarded as low temperature phases, and Cr3 has a high temperature phase. But this classification is somewhat arbitrary. The high temperature phase was observed even at room temperature in samples which were rapidly cooled. The low temperature phases (Cr1 and Cr2) were also found to coexist with the high temperature (Cr3) phase at elevated temperatures (see figure 4(*b*)).

An XRD scan of the liquid crystalline phase (140°C $< T <$ 150°C) is shown in figure 4(*e*), and is characterized by a sharp interlayer repeat of 22·2 Å, and an intense intralayer peak at 5·5 Å. Such a pattern is characteristic of S_B phase. Thus the XRD results are consistent with the optical microscopy identification of the S_B phase. The liquid crystalline phase occurs before the main melting peak. The isotropic phase (see figure 4(*f*)) has two amorphous halos at 24 and 6·6 Å which we attribute to interlayer and intralayer distances, respectively, in the (locally) nanophase-separated melt. The *d*-spacing of 22·2 Å observed for the S_B phase is less than the 28 Å calculated length of the molecule. One possibility is that the molecules are tilted with respect to the Bragg plane. To account for the absence of high-angle reflections it is further necessary to assume that such tilt is incoherent. However a fluid structure within the lamellae would give rise to diffuse interchain reflection, and not the fairly sharp 5·5 Å reflection that we observe. Therefore we suggest that

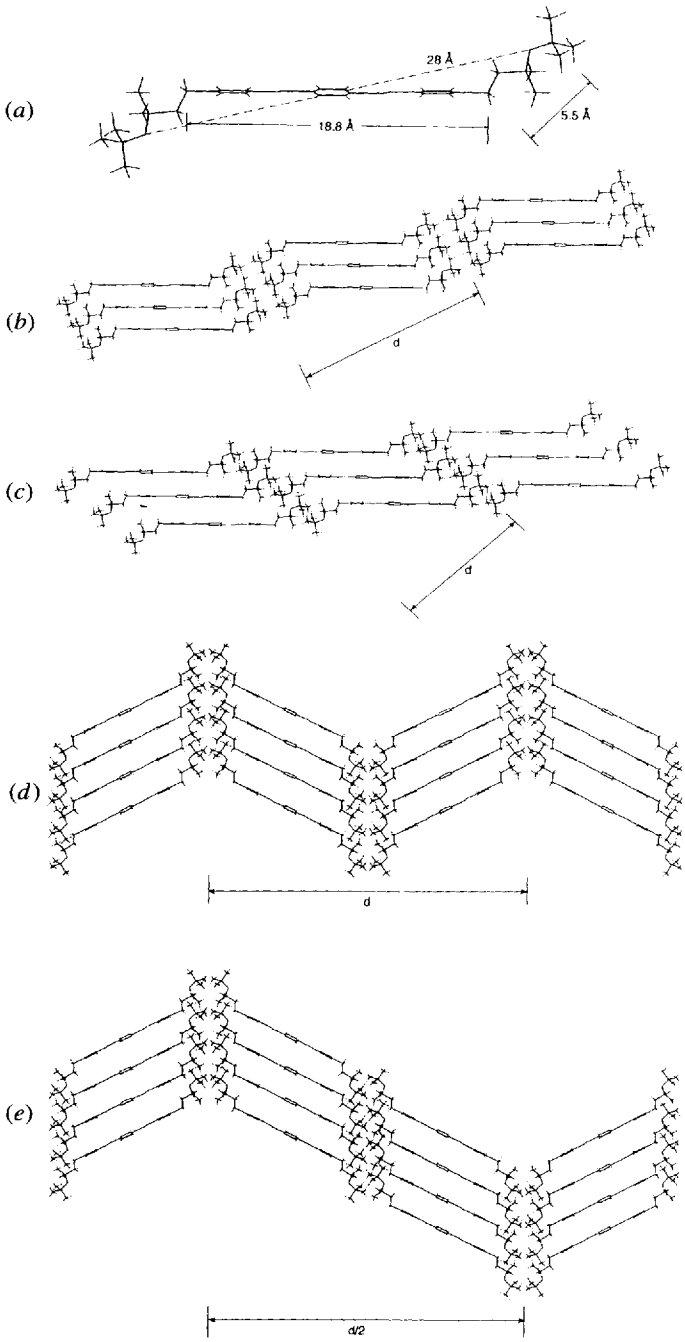

Figure 6. Structural models that account for the observed XRD results. (*a*) An edge-on view of an energy minimized molecular structure of TBS2A. (*b*) Disordered 29·5 Å single layer, Cr1 structure. (*c*) Single layer Cr2 and Cr3 structures in which siloxane chains form an interdigitized layer. (*d*) A speculative model for the 44 Å long spacing. (*e*) A speculative model for the 105 Å spacing.

Downloaded At: 09:41 26 January 2011

the observed *d*-spacing is smaller than the molecular length because of significant interdigitization of the siloxane tails (see figure 6 (*c*)).

The molecular packing of TBS2A shown in figures 6 (*b*) and (*c*), do not predict the observed long spacings (44–105 Å; Cr2 phase) which appear to be multiples of the monomer length. A crystalline phase with a chain-axis repeat which is a multiple (2 ×) of the chains-axis length has also been observed in TBBA [14], and is proposed for MBBA [15]. (Note that the orientation of the TBBA molecules in [14] is not zigzag as in figure 6 (*d*), and therefore this model does not provide a reflection with a spacing at 2 × the molecular repeat.) Similarly, lamellae repeats up to 7 chain-axis lengths have been observed in polyester amides where the multiple layers were assigned to the presence of rotational isomeric states in the adjacent layers of the smectic phase [16]. To account for the observed long spacings of 44–105 Å, we propose models in which the crystallographic repeating unit consists of two to four TBS2A layers as shown for instance in figures 6 (*d*) and (*e*). Such schemes also predict multilayers larger than the ones we report here.

4. Conclusions

The Schiff's base, *N*,*N*′-terephthalylidine-bis-4-vinylaniline (TBVA), which has a Cr–N transition at *c*. 180°C, is profoundly affected by the incorporation of di- and tri-siloxane tails. This substitution has been shown to reduce the transition temperatures and promote highly ordered smectic mesophases. The phase behaviour of the most robust siloxane mesogen, TBS2A, has been examined with DSC, microscopy, miscibility, and X-ray diffraction. These studies confirm that TBS2A exhibits a S_B phase. In TBS2A, there are at least two low temperature crystalline forms which upon heating give rise to a third crystalline form. The crystalline solid phase upon further heating transforms into a S_B liquid crystalline phase before reaching an isotropic melt phase. We suggest that the incompatibility between the siloxane moieties (tails) and the hydrocarbon mesogenic core underlies the adoption of multilayered structures.

We thank G. Chomyn for providing the DSC scan and W. B. Hammond for the use of the molecular modelling software. This work was supported in part by the Wright Patterson Materials Lab. under Air Force Prime Contract F3361-90-C-5813.

References

[1] Hsu, E. C., Kim, L. K., Blumstein, R. B., and Blumstein, A., 1976, *Molec. Crystals liq. Crystals*, **33,** 35.
[2] Clough, S. B., Blumstein, A., and Hsu, E. C., 1976, *Macromolecules*, **9,** 123.
[3] Braun, F., Willner, L., Hess, M., and Kosfeld, R., 1989, *Makromolek. Chem. rap. Commun.*, **10,** 51.
[4] Ozcayir, Y., Lai, X., Ratto, J., and Blumstein, A., 1990, *Molec. Crystals liq. Crystals*, **185,** 75.
[5] Bunning, T. J., Klei, H. E., Samulski, E. T., Crane, R. L., and Linville, R. J., 1991, *Liq. Crystals*, **10,** 445, and references therein.
[6] Drew, D., and Doyle, J. R., 1971, *Inorganic Synthesis*, edited by F. A. Cotton (McGraw-Hill, NY), Vol. 13, 47–56.
[7] Janini, G. M., Al-Ghoul, A. M., Hovakeemian, G. H., 1989, *Molec. Crystals liq. Crystals*, **172,** 69.
[8] Janini, G. M., Laub, R. J., and Shaw, T. J., 1985, *Makromolek. Chem. rap. Commun.*, **6,** 57.
[9] Aguilera, A., Bartulin, J., Hisgen, B., and Ringsdorf, H., 1979, *Makromolek. Chem.*, **184,** 253.
[10] Neubert, M. E., Ferrato, J. P., and Carpenter, R. E., 1979, *Molec. Crystals liq. Crystals*, **53,** 229.
[11] Shashidhar, R., 1990, Naval Research Lab., private communication.
[12] Gray, G. W., and Goodby, J. W. G., 1984, *Smectic Liquid Crystals* (Leonard Hill) .
[13] Ibid., p. 36.
[14] Doucet, J., Levelut, A. M., and Lambert, M., 1973, *Molec. Crystals liq. Crystals*, **24,** 317.
[15] Boese, R., Antipin, M. Yu., Nussbaumer, M., and Blaser, D., 1992, *Liq. Crystals*, **12,** 431.
[16] Murthy, N. S., and Aharoni, S. M., 1992, *Macromolecules*, **25,** 1177.

Downloaded At: 09:41 26 January 2011